The impact of soil microorganisms on the global budget of δ18O in atmospheric CO2

Lisa Wingate, Jérôme Ogée, Matthias Cuntz, Bernard Genty, Ilja Reiter, Ulli Seibt, Dan Yakir, Kadmiel Maseyk, Elise G. Pendall, Margatet M. Barbour, et al.

HAL Id: hal-02667878
https://hal.inrae.fr/hal-02667878

Submitted on 31 May 2020

The impact of soil microorganisms on the global budget of $\delta^{18}O$ in atmospheric CO_2

Lisa Wingate[a,b,1,2], Jérôme Ogée[b,1,2], Matthias Cuntz[c,1,3], Bernard Genty[d,e], Ilja Reiter[d,e], Ulli Seibt[f], Dan Yakir[g], Kadmiel Maseyk[f,g], Elise G. Pendall[h], Margaret M. Barbour[i], Behzad Mortazavi[j,k], Régis Burlett[b], Philippe Peylin[f], John Miller[l,m], Maurizio Mencuccini[a], Jee H. Shim[n], John Hunt[i], and John Grace[a]

[a]School of GeoSciences, University of Edinburgh, Edinburgh EH9 3JN, United Kingdom; [b]Unité de Recherche 1263 Ecologie Fonctionnelle et Physique de l'Environnement, Institut National de la Recherche Agronomique, 33130 Villenave d'Ornon, France; [c]Max Planck Institute for Biogeochemistry, 07701 Jena, Germany; [d]Laboratoire d'Ecophysiologie Moléculaire des Plantes, Institut de Biologie Environnementale et de Biotechnologie, Service de Biologie Végétale et de Microbiologie Environnementale, Commissariat à l'Energie Atomique, 13108 Saint-Paul-lez-Durance, France; [e]Unité Mixte de Recherche Biologie Végétale et Microbiologie Environnementales, Centre National de la Recherche Scientifique, 13108 Saint-Paul-lez-Durance, France; [f]Unité Mixte de Recherche 7618 Biogéochimie et Ecologie des Milieux Continentaux, Centre National de la Recherche Scientifique/Université Pierre et Marie Curie, 78850 Thivernal-Grignon, France; [g]Department of Environmental Sciences and Energy Research, Weizmann Institute of Science, Rehovot, 76100, Israel; [h]Department of Botany, University of Wyoming, Laramie, WY 82071; [i]Landcare Research, P.O. Box 40, Lincoln 7640, New Zealand; [j]Department of Biological Sciences, University of Alabama, Tuscaloosa, AL 35487; [k]Dauphin Island Sea Lab, Dauphin Island, AL 36528; [l]National Oceanic and Atmospheric Administration Earth System Research Laboratory, 325 Broadway R/GMD1, Boulder, CO 80305; [m]Cooperative Institute for Research in Environmental Sciences, University of Colorado, Boulder, CO 80309; and [n]Department of Forest, Rangeland, and Watershed Stewardship, Colorado State University, Fort Collins, CO 80523

Improved global estimates of terrestrial photosynthesis and respiration are critical for predicting the rate of change in atmospheric CO_2. The oxygen isotopic composition of atmospheric CO_2 can be used to estimate these fluxes because oxygen isotopic exchange between CO_2 and water creates distinct isotopic flux signatures. The enzyme carbonic anhydrase (CA) is known to accelerate this exchange in leaves, but the possibility of CA activity in soils is commonly neglected. Here, we report widespread accelerated soil CO_2 hydration. Exchange was 10–300 times faster than the uncatalyzed rate, consistent with typical population sizes for CA-containing soil microorganisms. Including accelerated soil hydration in global model simulations modifies contributions from soil and foliage to the global $CO^{18}O$ budget and eliminates persistent discrepancies existing between model and atmospheric observations. This enhanced soil hydration also increases the differences between the isotopic signatures of photosynthesis and respiration, particularly in the tropics, increasing the precision of CO_2 gross fluxes obtained by using the $\delta^{18}O$ of atmospheric CO_2 by 50%.

carbon cycle | water cycle | carbonic anhydrase | oxygen isotopes | terrestrial biosphere

The Earth's climate system is intimately connected to the movement of water and carbon across the planetary surface. As global warming proceeds, it is expected that photosynthetic CO_2 uptake will increase in colder regions of the world and diminish in those regions that are already warm and dry (1). At the same time, warming is expected to increase microbial activity, at least where water is not limiting, and therefore lead to an enhanced breakdown of organic matter in the soil, producing a large respiratory flux of CO_2 back to the atmosphere (2). Because terrestrial ecosystems presently sequester about a quarter of the CO_2 emissions associated with fossil fuel burning $(7.1 \, GtC \, y^{-1})$ (1), it is critical that we understand how large-scale, climate-driven changes will affect the carbon sequestration of the terrestrial biosphere. Currently, the precise response of terrestrial CO_2 sources and sinks to changes in climate remains uncertain (3) and its understanding requires the ability to quantify the amount of CO_2 taken up during photosynthesis separately from the amount released by respiration.

The oxygen isotope composition of atmospheric CO_2 (δ_a) was shown to be a powerful tracer of photosynthetic and respiratory CO_2 fluxes while at the same time providing information on the intensity of water cycling within terrestrial ecosystems (4–6). This tracing property occurs because the oxygen isotope composition ($\delta^{18}O$) of leaf and soil water pools is transferred to atmospheric CO_2 during photosynthetic and respiratory CO_2 exchange, via an isotopic exchange during CO_2 hydration (7): $CO_{2aq} + H_2^{18}O \leftrightharpoons CO^{18}O_{aq} + H_2O$. Despite the short residence time of CO_2 in leaves, CO_2 involved in photosynthesis is nearly completely relabeled by ^{18}O-enriched leaf water because of the enzyme carbonic anhydrase (CA; EC 4.2.1.1), a very efficient catalyst of CO_2 hydration and isotopic exchange (4, 5, 8, 9). Typically the $\delta^{18}O$ of leaf and soil water pools are very different. There is a tendency for the heavier molecules of water to accumulate more readily in leaves than in soils during evapotranspiration because of the difference in water pool size (10, 11). Because the CO_2–H_2O exchange in leaves (associated with photosynthesis) or soils (associated with soil respiration) produces such contrasting ^{18}O signals, estimates of the amount of CO_2 exchanged during photosynthesis and respiration can in principle be constrained by using the $\delta^{18}O$ signal of atmospheric CO_2 (6, 12).

However, our ability to partition gross fluxes of CO_2 may be complicated because the $\delta^{18}O$ of soil water (δ_{sw}) can often display a strong vertical gradient at the soil surface because soil evaporation also leads to an enrichment of heavy water molecules in the uppermost layers (13–15). Thus, to determine the $\delta^{18}O$ of CO_2 exchanged between soils and the atmosphere accurately it becomes necessary to know the shallowest depth (z_{eq}) where diffusing CO_2 molecules (from the atmosphere or produced by soil respiration; Fig. 1A) have enough time to fully equilibrate isotopically with soil water. With increasing temperature and moisture, CO_2 hydration increases relative to the diffusion rate so that z_{eq} moves closer to the surface, and toward more enriched $\delta^{18}O$ values (see *Methods*, Eq. **4**). Although we know that CA accelerates the rate of hydration in leaves, the possibility of CA activity in soils is commonly neglected (4, 15),

GEOPHYSICS

MICROBIOLOGY

Fig. 1. Schematic showing the influence of CO_2 hydration rates on vertical profiles of $\delta^{18}O$ in soil air CO_2. (*A*) The net soil-atmosphere CO_2 exchange is composed of CO_2 molecules moving from the atmosphere into the soil and back to the atmosphere (i.e., invasion) and further CO_2 molecules produced during soil respiration. Because of oxygen isotopic exchange between soil CO_2 and water, both invasion and respiration fluxes modify the isotopic composition of atmospheric CO_2, and their ^{18}O isotopic signature depend on the extent of CA activity in the soil. (*B*) Typical profile of $\delta^{18}O$ in soil air CO_2 (δ_{sa}) for uncatalyzed CO_2 hydration in soil water (enhancement factor $f_{CA} = 1$). (*C*) Same as in *B* but for catalyzed CO_2 hydration (enhancement factor $f_{CA} \gg 1$). In deep soil layers where vertical gradients of δ_{sw} are weak, the residence time of CO_2 is long enough to reach full isotopic equilibrium with soil water ($\delta_{sa} = \delta_{sw} - \varepsilon_{eq}$), where ε_{eq} denotes the isotopic equilibrium fractionation between CO_2 and water (22). Above a certain depth z_{eq} (where, by definition, $\delta_{sa} = \delta_{eq}$), CO_2 molecules diffuse too rapidly to fully equilibrate with local soil water. If CO_2 hydration is enhanced because of CA activity ($f_{CA} \gg 1$), the equilibration becomes faster and z_{eq} shallower, thus δ_{eq} becomes more enriched.

because the abundance and location of CA in soils is still somewhat unclear, with only indirect and isolated indications based on measurements of $\delta^{18}O$ of soil CO_2 or COS fluxes (14, 16, 17). Substantial CA activity in soils would lead to a faster equilibration of CO_2, moving z_{eq} further toward the surface where soil water is more ^{18}O enriched (Fig. 1 *B* and *C*). So far global simulations have assumed uncatalyzed CO_2 hydration in soils (18–20) and equilibration depths below the region of strong evaporative enrichment (5, 21).

Results and Discussion

Evidence for Enhanced Soil CO_2 Hydration Rates. Here, we demonstrate that, in contrast to current assumptions, the observed rate of soil CO_2 hydration is always substantially faster than the uncatalyzed rate. We compared measurements of depth-resolved soil water $\delta^{18}O$ (δ_{sw}) and observed $\delta^{18}O$ signatures of chamber-based soil CO_2 fluxes (δ_{flux}) in seven different ecosystems that encompass most of the major land biomes, providing a global perspective of ^{18}O exchange in soils (Table S1 and see Tables S5–S7). From the δ_{sw} data, we determined the depth-resolved $\delta^{18}O$ of soil CO_2 in full equilibrium with soil water (δ_{eq}), equal to $\delta_{sw} - \varepsilon_{eq}$ where ε_{eq} is the temperature-sensitive equilibrium fractionation between CO_2 and water (22). Most sites exhibited strong gradients in $\delta_{sw} - \varepsilon_{eq}$ at the soil surface, reflecting the evaporative enrichment of soil water (Fig. 2). From the δ_{flux} data, we determined the $\delta^{18}O$ of soil CO_2 at z_{eq} (δ_{eq}, see Fig. 1) for different rates of hydration expressed as an enhancement factor (f_{CA}) with respect to the uncatalyzed CO_2 hydration rate (see Eq. **6** in *Methods*). Increasing f_{CA} shifts z_{eq} toward surface layers (Fig. 2) and δ_{eq} toward δ_a. The best estimate for f_{CA} would be one in agreement with both soil water and chamber flux measurements. This is obtained when the point (δ_{eq}, z_{eq}) derived from the chamber data intersects the δ_{eq} curve derived from soil water measurements. At all sites, this intersection occurs for values of f_{CA} between 10 and 300, with the lowest f_{CA} in the cooler temperate ecosystems while higher f_{CA} were found at the Mediterranean and subtropical sites (Fig. 2). As a consequence, the equilibration depth z_{eq} was in most cases within the top 5 cm of the soil, the zone containing the strongest δ_{sw} gradients. A reduction in the effective diffusivity of soil CO_2 would also lead to shallower equilibration depths z_{eq} by increasing the residence time of CO_2 in soils, but it would not yield simultaneous solutions for both soil water and CO_2 flux isotope data (14). Thus, an enhanced CO_2 hydration rate is the only plausible mechanism to explain these chamber-based measurements.

Consistency with CA Activities in Soil Microorganisms. The uppermost soil layers host many bacterial, algal, and fungal species that produce intracellular and sometimes extracellular CAs (23–25). Based on a literature survey, we claim that this mixed population

Fig. 2. The $\delta^{18}O$ of soil CO_2 at the depth of full equilibration (δ_{eq}, z_{eq}; see Fig. 1) estimated from chamber flux measurements for different levels of hydration rates (f_{CA}). Depth-resolved soil water data yields the $\delta^{18}O$ of CO_2 in isotopic equilibrium with soil water ($\delta_{sw} - \varepsilon_{eq}$). The point at which the two curves intersect indicates the most likely value for the enhancement factor, f_{CA}, listed below the ecosystem type for each site (see Table S1). The horizontal error bars on the squared symbols represent the standard deviation of δ_{eq} values over the number of δ_{flux} measurements ($n = 1$–15).

of soil microorganisms is responsible for the accelerated soil CO_2 hydration. Most soils contain 10^3 to 10^6 algae per g of dry soil, but populations can reach 10^8 algae per g of dry soil (Table S2). Bacterial population sizes are even larger at 10^8 to 10^9 cells per g of dry soil (Table S3). At 25 °C, the CO_2 hydration rate in soil algal and cyanobacterial cells can be up to 172,500 times the uncatalyzed rate, comparable to CA activities found in plant chloroplasts (Table S4). With a cell volume of ≈ 100 μm^3 and population of 10^6 per g of dry soil, algae could explain a significant fraction of our observed soil CA activities. Indeed, we found that the presence of algae developing naturally on the surface of a peat soil dramatically enhanced CA activity (Table S4). Laboratory studies have also reported high CA activities ($f_{CA} = 50$) in bulk soil extracts from subtropical karst forests containing a mixture of bacterial and fungal species (Table S4). Based on a cell volume of ≈ 1 μm^3 and population of 4×10^9 cells per g of dry soil (Table S3), this soil-level f_{CA} value would be consistent with soil bacteria operating at a cell-level CO_2 hydration of 8,000 times the uncatalyzed rate (Table S4). These estimates demonstrate that soil microorganisms are likely to be responsible for enhanced soil CO_2 hydration rates of 20–300 times the uncatalyzed rate.

Impact of Soil CA Activity at the Global Scale. The accelerated hydration of CO_2 in soils has been missing in the mass budget of $\delta^{18}O$ in atmospheric CO_2. To explore the impact of soil CA activity on the $\delta^{18}O$ of atmospheric CO_2, and its north–south (N-S) gradient, we incorporated this biological process into the global model of $\delta^{18}O$ in atmospheric CO_2, Mecbeth (18, 19) (see *Methods*). Simulations were performed over an average year calculated from the 1990s and compared with observations from the worldwide network of atmospheric stations for the same decade (26, 27). Three scenarios are discussed here: one uncatalyzed (abiotic) scenario ($f_{CA} = 1$) and two globally uniform f_{CA} scenarios covering the range of soil chamber estimates ($f_{CA} = 20$ and $f_{CA} = 300$).

The high CA activity scenario ($f_{CA} = 300$) improves the agreement between the modeled and observed N-S gradient in δ_a, particularly when compared with the uncatalyzed, abiotic scenario (Fig. 3). This latitudinal feature in δ_a is largely driven by the N-S gradient in the $\delta^{18}O$ of precipitation that creates depleted leaf and soil water pools toward the northern latitudes. In the uncatalyzed scenario ($f_{CA} = 1$), photosynthesis dominates the N-S gradient. Introducing f_{CA} enhances the invasion flux (the number of CO_2 molecules from the atmosphere that equilibrate with soil water and go back to the atmosphere; see Fig. 1A and *Methods*, Eq. 5). The contribution of this invasion flux to the N-S gradient increases with f_{CA} and at some latitudes becomes larger than the contribution of respiration.

Incorporating high CA activity ($f_{CA} = 300$) also reduces the mean value of δ_a by $\approx 1\%$ relative to the abiotic case ($f_{CA} = 1$), bringing the model closer to atmospheric observations. This reduction is the result of complex interactions between δ_a and the $\delta^{18}O$ signatures of all component fluxes. The influence of each process on δ_a can be represented by using the concept of isoflux (I_x) defined as the product of a gross CO_2 flux (F_x) and its isotopic composition (δ_x) relative to δ_a: $I_x = F_x (\delta_x - \delta_a)$. Photosynthesis tends to enrich the atmosphere (positive isoflux, $\delta_x > \delta_a$), whereas respiration and soil invasion usually have the opposite effect (negative isoflux, $\delta_x < \delta_a$). Nonbiospheric fluxes (from ocean, fossil fuel, and biomass burning) also tend to deplete δ_a, but to a much lesser extent (19, 28). In the uncatalyzed scenario ($f_{CA} = 1$), photosynthetic (I_A), and respiratory (I_R) isofluxes balance the nonbiospheric isofluxes globally while the soil invasion isoflux (I_{inv}) remains close to zero at all latitudes (Fig. 3). When f_{CA} is increased, the isotopic signatures of soil invasion and respiration become progressively enriched as a result of the isotopic gradient in δ_{sw} (Fig. 1), but usually remain

Fig. 3. Simulated contributions of different biospheric processes to the N-S gradient in δ_a for uncatalyzed ($f_{CA} = 1$) or enhanced ($f_{CA} \gg 1$) CO_2 hydration rates in the soil, compared with measured δ_a. Enhanced hydration increases the corresponding isofluxes of soil invasion and photosynthesis + respiration, i.e., the isotopic imbalance required for gross flux partitioning. Note that δ_a values are always reported relative to the South Pole and thus do not show the absolute changes in δ_a (−0.1‰ and −1.1‰ for f_{CA} of 20 and 300 relative to $f_{CA} = 1$, respectively).

below δ_a (I_R and I_{inv} remain negative). Most importantly, the mass of atmospheric CO_2 molecules that equilibrate with soil water increases from 25 GtC yr^{-1} in the uncatalyzed scenario to 450 GtC yr^{-1} when $f_{CA} = 300$. As a result, I_{inv} becomes very large and negative, reaching nearly the same magnitude as soil respiration. The associated depletion in δ_a is partly compensated by an increase in both I_A and I_R. When $f_{CA} = 300$, the absolute value of I_{inv} increases by 571 GtC ‰ yr^{-1}, whereas I_R decreases by 226 GtC ‰ yr^{-1} and I_A increases by 269 GtC ‰ yr^{-1}. Soil CA activity thus strongly modifies the relative contribution of photosynthesis and respiration to the $CO^{18}O$ budget in our global model.

Consequences for the Retrieval of CO_2 Sources and Sinks. Measurements of δ_a have been proposed as one of the few tools available to partition net CO_2 fluxes into photosynthesis and soil respiration, but it critically depends on the existence of sufficient imbalance between I_A and I_R (4–6, 9, 12, 21, 28). In previous studies, where δ_a was prescribed and not dynamically coupled to soil and leaf water pools as in our study, such an imbalance had been restricted to the boreal regions (5, 21, 28). In contrast, we now show a significant isotopic imbalance at nearly all latitudes (photosynthesis + respiration curve in Fig. 3), greatly enhancing the potential of the ^{18}O approach for partitioning CO_2 fluxes. At the continental scale, there is a strong isotopic imbalance over Europe and North America coinciding with the peak season of photosynthetic activity in the Northern Hemisphere (Fig. 4). Over the tropics, the isotopic imbalance between I_A and I_R increases by up to 50% when $f_{CA} = 300$ and is maintained year-round in many areas (Fig. 4). The uncertainties of tropical gross CO_2 fluxes could thus be reduced by an equivalent amount (12), making the $\delta^{18}O$ of atmospheric CO_2 a better tracer for terrestrial gross CO_2 fluxes than previously thought in these regions. From a one-box global mass balance budget and using globally averaged fluxes and isotopic signatures from Mecbeth, we calculated that, neglecting "biotic" invasion associated with soil CA activity in inversion studies leads to errors in the isotope-derived estimates of global photosynthesis by up to 30 GtC yr^{-1}, i.e., $\approx 30\%$ of current estimates (1).

June   **December**

-30 -20 -10 0 10 20 30 40 50 60 70

Isotopic Imbalance $I_A + I_R$

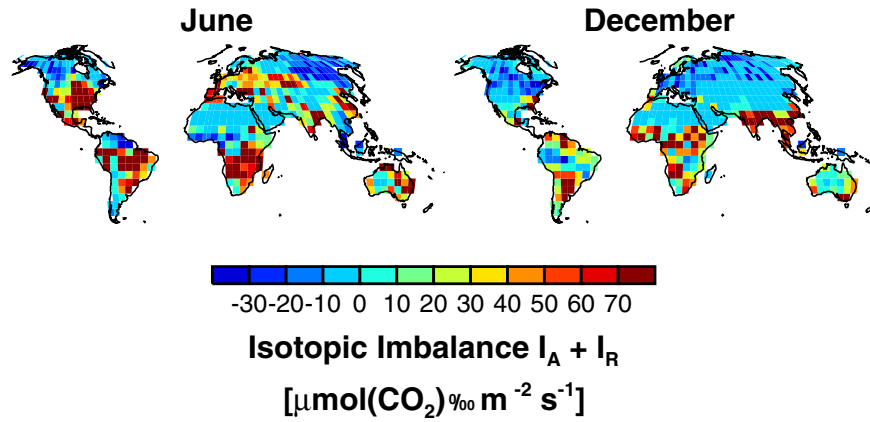**[μmol(CO$_2$)‰ m^{-2} s^{-1}]**

Fig. 4. Global distribution in the extent of isotopic imbalance ($I_A + I_R$) across continental surfaces for June and December simulated by the global model Mecbeth for the most enhanced soil CO$_2$ hydration scenario ($f_{CA} = 300$). Regions where $I_A + I_R$ is the most different from zero correspond to regions of strong isotopic imbalance where biospheric gross CO$_2$ fluxes are expected to be the most constrained by δ^{18}O data.

Future Directions for Global Isotope-Enabled Models. This study demonstrates that enhanced rates of CO$_2$ hydration occur at the soil surface and appreciably impact the oxygen isotope composition of atmospheric CO$_2$. This enhanced exchange in the soil brings into focus our limited ability to predict the isotopic enrichment of soil water near the surface (18, 29), highlighting a need for future improvements in this research area. Also, although we provided the basic observations and parameterization, more work is now needed to further assess the variability in f_{CA} in different ecosystems, plant functional types, or regions within the global model, including attempts to establish the mechanistic basis to underpin the observed differences in CA activity between ecosystems. Developments on these fronts will greatly enhance our capabilities to use the δ^{18}O of atmospheric CO$_2$ to quantitatively inform us of large-scale changes in the intensity of carbon and water cycling in terrestrial ecosystems.

Methods

Soil CO^{18}O Budget Equation. In a given soil layer, the number of moles of CO^{18}O changes as a result of (*i*) CO^{18}O production during heterotrophic and autotrophic respiration, (*ii*) diffusion of these molecules through the soil layer, and (*iii*) oxygen isotopic exchange with the surrounding soil water (30–32):

$$\theta_t \frac{\partial C \mathcal{R}}{\partial t} = \mathcal{R}_c S_c + \frac{\partial}{\partial z}\left[D_{c,iso} \frac{\partial C \mathcal{R}}{\partial z} \right] + k_{h,iso} B \theta_w C (\mathcal{R}_{eq} - \mathcal{R}),$$

[1]

where C [mol·mol^{-1}] is the CO$_2$ mole fraction in soil air, $\mathcal{R}$, $\mathcal{R}_c$, and $\mathcal{R}_{eq}$ are the ^{18}O/^{16}O ratios of the CO$_2$ in soil air, respired CO$_2$, and CO$_2$ in isotopic equilibrium with the surrounding soil water, respectively, S_c (mol·m^{-3}·s^{-1}) is the respiration rate density, $D_{c,iso}$ (m^2·s^{-1}) is the effective diffusivity of CO^{18}O in soil air, θ_w (m^3·m^{-3}) is the volumetric soil water content, B is the CO$_2$ solubility coefficient, and θ_t (m^3·m^{-3}) is the total CO$_2$ porosity. Denoting by θ_a the soil air porosity we have (31): $\theta_t = \theta_a + B\theta_w$. The solubility coefficient B depends on soil temperature T_s (K) according to ref. 33: $B = 1.739\exp(-0.039(T_s - 273.15) + 0.000236(T_s - 273.15)^2)$. $\mathcal{R}_{eq}$ is related to the ^{18}O/^{16}O ratio in soil water $\mathcal{R}_{sw}$ through $\mathcal{R}_{eq} = (1 + \varepsilon_{eq}) \mathcal{R}_{sw}$, where $\varepsilon_{eq} = 17.604/T_s - 0.01793$ is the CO$_2$–H$_2$O equilibrium fractionation (22). Because there are three oxygen atoms present in the bicarbonate intermediate, the isotopic exchange rate during CO$_2$ hydration equals one-third the hydration rate (7): $k_{h,iso} = f_{CA}k_{h,uncat}/3$, where (34) $k_{h,uncat} = 0.037 \times \exp(0.118(T_s - 298.15))$. In this framework, CA activity is expressed as an enhancement factor (f_{CA}) of the uncatalyzed CO$_2$ hydration rate ($k_{h,uncat}$). The effective CO^{18}O diffusivity in soil air is calculated as $D_{c,iso} = D_{c,eff} \alpha_d$, where $\alpha_d = 0.9913$ is the isotopic discrimination during molecular diffusion of CO$_2$ in air and $D_{c,eff}$ (m^2·s^{-1}) is the effective CO$_2$ diffusivity in soil air. Several parameterizations of this effective diffusivity exist in the literature that differ mostly for wet soils (35). Results presented in this study use ref. 31: $D_{c,eff} = 0.66 \times \theta_a \times 1.4 \cdot 10^{-5} (T_s/298.15)^{1.75}$.

Full Equilibration Depth. The budget equation above contains two time scales. One time scale indicates the half-life of CO$_2$ molecules before being isotopically equilibrated with the surrounding water:

$$\tau_k = \ln 2 \cdot \left(\frac{\theta_t}{k_{h,iso} B \theta_w} \right)$$

[2]

and another time scale indicates the time required for a plume of C^{18}OO molecules to diffuse through the soil over a given distance z:

$$\tau_d(z) = \frac{\theta_t z^2}{2 D_{c,iso}}.$$

[3]

Full equilibration within a soil layer of thickness z is satisfied when the time scale for isotopic equilibration is smaller than the time scale for diffusion through this layer, i.e., $\tau_k \ll \tau_d(z)$. When $\tau_k = \tau_d(z)$, full equilibration can occur if the soil layer has uniform soil temperature, moisture content, and isotopic composition. However, in the top centimeters of the soil, strong gradients of T_s, θ_w, and $\mathcal{R}_w$ are more likely. The shallowest depth of full equilibration, z_{eq}, must therefore satisfy the inequality: $\tau_k < \tau_d(z_{eq})$. In the following we will define z_{eq} as: $\tau_k = \tau_d(z_{eq})/4$, or similarly:

$$z_{eq} = 2\sqrt{\frac{2\ln 2 D_{c,iso}}{k_{h,iso} B \theta_w}}.$$

[4]

The factor 4 was determined by matching the value of f_{CA} deduced in Fig. 2 with that obtained from simulations using the full numerical model (Eq. **1**), i.e., $f_{CA} \approx 300$ for the Mediterranean evergreen site (14) and $f_{CA} \approx 20$ for the montane evergreen site (15). Eq. **4** with $f_{CA} = 20$ also provides seasonal variations of z_{eq} at the temperate evergreen site that correspond to the depth where δ^{18}O in soil air CO$_2$ (δ_{sa}) and $\delta_{sw} - \varepsilon_{eq}$ (estimated using the full numerical model, Eq. **1**) start to diverge by >0.3 ‰ (a threshold chosen for practical purposes to represent the overall precision of soil water isotope measurements).

Other studies (14, 35) use a different formulation for $D_{c,iso}$, leading to values of this diffusivity 5-fold smaller in saturated soils. Using this other formulation does not fundamentally change the results presented in Fig. 2.

Soil CO$_2$ Isoflux. In the steady state, and assuming isothermal and uniform soil water conditions, Eq. **1** can also be solved analytically (30–32). In this framework, the isotopic composition of the soil CO$_2$ flux δ_{flux} is:

$$\delta_{flux} = \delta_{eq} + \varepsilon_{d,eff} + (\delta_{eq} - \delta_a)v_{inv}\frac{C_a}{F_R},$$

[5]

where $\varepsilon_{d,eff}$ is the effective isotopic fractionation during diffusion, F_R is the soil CO$_2$ efflux, and $v_{inv} = \sqrt{B\theta_w k_{h,iso} D_{c,iso}}$ has the dimensions of a velocity (m·s^{-1}) that when multiplied by C_a gives the soil invasion flux F_{inv}. The product ($\delta_{flux} - \delta_a$)F_R is called the soil CO$_2$ isoflux. It can be seen as the sum of two isotope fluxes: a respiration isoflux, $I_R = (\delta_{eq} + \varepsilon_{d,eff} - \delta_a)F_R$, and an invasion isoflux, $I_{inv} = (\delta_{eq} - \delta_a)F_{inv}$, sometimes defined as abiotic because it is independent of

F_R. Assuming a uniform soil CO_2 production S_c over a soil column of depth z_0, $\varepsilon_{d,eff}$ can be estimated as (31): $\varepsilon_{d,eff} = \varepsilon_d(1 - z_1/z_0(1 - \exp(-z_0/z_1)))$, where $z_1 = (2\sqrt{2\ln2})^{-1} z_{eq}$. Eq. 5 can then be inverted to estimate δ_{eq} as a function of δ_{flux}, C_a, δ_a, and F_R measurements:

$$\delta_{eq} = \frac{\delta_{flux} - \varepsilon_{d,eff} + v_{inv}C_a/F_R\delta_a}{1 + v_{inv}C_a/F_R}. \qquad [6]$$

Oxygen Isotope Composition of the Net CO_2 Flux from Soil Chambers. The steady-state oxygen isotope signal of the net soil CO_2 flux during chamber closure (δ_{ch}) was calculated by using a simple isotopic mass balance:

$$\delta_{ch} = \frac{\delta_{out}C_{out} - \delta_{in}C_{in}}{C_{out} - C_{in}}, \qquad [7]$$

where C_{out}, C_{in} and δ_{out}, δ_{in} are the mole fractions and isotopic compositions of CO_2 in the air leaving and entering the chamber, respectively. In the case of the two sites that used closed chambers (subtropical evergreen and semiarid grassland), C_{out}, C_{in} and δ_{out}, δ_{in} are the mole fractions and isotopic compositions of CO_2 at the start and end of a defined chamber closure period, respectively.

To derive δ_{eq} values from soil chamber data, we use Eq. 6, neglect chamber effects, and make the common assumption that the atmosphere inside the chamber is well mixed ($C_a = C_{out}$ and $\delta_a = \delta_{out}$).

Oxygen Isotope Composition of Soil Water. Depth-resolved soil samples were collected at each experimental site within proximity of the soil chamber and at approximately the same time as gas exchange measurements. In the case of the Mediterranean evergreen, subtropical evergreen, and both temperate ever- green sites, soil water was extracted cryogenically from bulk soil samples and $\delta^{18}O$ analysis of CO_2 equilibrated with the extracted water was completed (14). For the montane evergreen, subtropical deciduous, and semiarid grassland sites CO_2 with a known isotopic composition was equilibrated directly with fresh soil samples and stored in gas-tight containers for 12 h. Equilibrated CO_2 was then sampled from the container and analyzed for its $\delta^{18}O$ composition (15).

Global Model Simulations. The global model Mecbeth calculates the sources and sinks of CO_2, water, and their respective isotopes and transports them in the atmosphere (18, 19). It merges a description of the biospheric energy, water, and carbon fluxes with a global climate and water isotope model. The atmosphere and biosphere are dynamically coupled to account for feedbacks of the accelerated equilibration of CO_2 with soil water on δ_a and the isotopic signatures of leaf and other fluxes. The model parameterization of soil water isotopes was improved in this study to provide depth-resolved descriptions of soil water and soil water isotopes (35), a necessary step if CA activity occurs in soils containing strong vertical gradients in δ_{sw} (14). Several soil layers of varying thickness were included in the model. The most important upper layers relevant to this study consisted of a top layer at 0–6 cm and another layer at 6–20 cm.

1. Intergovernmental Panel on Climate Change (2007) *Climate Change 2007–The Physical Sciences Basis: Contribution of Working Group I to the Fourth Assessment Report of the Intergovernmental Panel on Climate Change* (Cambridge Univ Press, Cambridge, UK).
2. Davidson EA, Janssens IA (2006) Temperature sensitivity of soil carbon decomposition and feedbacks to climate change. *Nature* 440:165–173.
3. Friedlingstein P, et al. (2006) Climate-carbon cycle feedback analysis: Results from the C⁴MIP model intercomparison. *J Clim* 19:3337–3353.
4. Francey RJ, Tans PP (1987) Latitudinal variation in oxygen-18 of atmospheric CO_2. *Nature* 327:495–497.
5. Farquhar GD, et al. (1993) Vegetation effects on the isotope composition of oxygen in atmospheric CO_2. *Nature* 363:439–443.
6. Yakir D, Wang X-F (1996) Fluxes of CO_2 and water between terrestrial vegetation and the atmosphere estimated from isotope measurements. *Nature* 380:515–517.
7. Mills GA, Urey HC (1940) The kinetics of isotopic exchange between carbon dioxide, bicarbonate ion, carbonate ion and water. *J Am Chem Soc* 62:1019–1026.
8. Silverman DN (1982) Carbonic anhydrase: Oxygen-18 exchange catalyzed by an en- zyme with rate-contributing proton-transfer steps. *Methods Enzymol* 87:732–752.
9. Gillon JS, Yakir D (2001) Influence of carbonic anhydrase activity in terrestrial vegeta- tion on the ^{18}O content of atmospheric CO_2. *Science* 291:2584–2587.
10. Dongmann G, Nürnberg HW, Förstel H, Wagener K (1974) On the enrichment of $H_2^{18}O$ in the leaves of transpiring plants. *Radiat Environ Biophys* 11:41–52.
11. Farquhar GD, Cernusak LA, Barnes B (2007) Heavy water fractionation during transpi- ration. *Plant Physiol* 143:11–18.
12. Ogée J, et al. (2004) Partitioning net ecosystem carbon exchange into net assimi- lation and respiration with canopy-scale isotopic measurements: An error propa- gation analysis with $^{13}CO_2$ and $CO^{18}O$ data. *Global Biogeochem Cycles*, 2010.1029/ 2003GB002166.
13. Barnes CJ, Allison GB (1988) The distribution of deuterium and oxygen-18 in dry soils: I. Theory. *J Hydrol* 60:141–156.
14. Wingate L, et al. (2008) Oxygen stable isotope signals of net soil CO_2 efflux record changes in soil evaporation and indicate the presence of carbonic anhydrase in Mediterranean soils. *Global Change Biol* 14:2178–2193.
15. Miller JB, Yakir D, White JMC, Tans PP (1999) Measurements of $^{18}O/^{16}O$ in the soil- atmosphere CO_2 flux. *Global Biogeochem Cycles* 13:761–774.
16. Seibt U, Wingate L, Lloyd J, Berry J (2006) Diurnally variable $\delta^{18}O$ signatures of soil CO_2 fluxes indicate carbonic anhydrase activity in a forest soil. *J Geophys Res*, 10.1029/ 2006JG000177.
17. Kesselmeier J, Teusch N, Kuhn U (1999) Controlling variables for the uptake of atmospheric carbonyl sulfide by soil. *J Geophys Res* 104:11577–11584.
18. Cuntz M, et al. (2003) A comprehensive global three-dimensional model of $\delta^{18}O$ in atmospheric CO_2: 2. Mapping the atmospheric signal. *J Geophys Res*, 45101029/ 2002JD003154:002003.
19. Cuntz M, Ciais P, Hoffmann G, Knorr W (2003) A comprehensive global three- dimensional model of $\delta^{18}O$ in atmospheric CO_2: 1. Validation of surface processes. *J Geophys Res*, 4510.1029/2002JD003153.
20. Stern L, Amundson R, Baisden WT (2001) Influence of soils on oxygen isotope ratio of atmospheric CO_2. *Global Biogeochem Cycles* 15:753–759.
21. Peylin P, et al. (1999) A 3-dimensional study of $\delta^{18}O$ in atmospheric CO_2: Contribution of different land ecosystems. *Tellus* 51B:642–667.
22. Brenninkmeijer CAM, Kraft P, Mook WG (1983) Oxygen isotope fractionation between CO_2 and water. *Isotope Geosci* 1:181–190.
23. Smith KS, Ferry JG (2000) Prokaryotic carbonic anhydrases. *FEMS Microbiol Rev* 24:335– 366.
24. Badger MR, Price GD (1994) The role of carbonic anhydrase in photosynthesis. *Annu Rev Plant Physiol Plant Mol Biol* 45:369–392.
25. Moroney JV, Bartlett SG, Samuelsson G (2000) Carbonic anhydrases in plants and algae. *Plant Cell Environ* 24:141–153.
26. Trolier M, White JWC, Tans PP, Masarie KA, Gemery PA (1996) Monitoring the isotopic composition of atmospheric CO_2: Measurements from the NOAA global air sampling network. *J Geophys Res* 101:25897–25916.
27. Allison CE, Francey RJ (2007) Verifying Southern Hemisphere trends in atmospheric carbon dioxide stable isotopes. *J Geophys Res*, 21310.21029/22006JD000734.
28. Ciais P, et al. (1997) A three-dimensional synthesis study of $\delta^{18}O$ in atmospheric CO_2. 1. Surface fluxes. *J Geophys Res* 102:5857–5872.
29. Cornwell AR, Harvey LDD (2007) Soil moisture: A residual problem underlying AGCMs. *Clim Change* 84:313–336.
30. Hesterberg R, Siegenthaler U (1991) Production and stable isotopic composition of CO_2 in a soil near Bern, Switzerland. *Tellus* 43:197–205.
31. Tans PP (1998) Oxygen isotopic equilibrium between carbon dioxide and water in soils. *Tellus* 50:163–178.
32. Amundson R, Stern L, Baisden WT, Wang Y (1998) The isotopic composition of soil and soil-respired CO_2. *Geoderma* 82:83–114.
33. Weiss RF (1974) Carbon dioxide in water and seawater: The solubility of nonideal gas. *Mar Chem* 2:203–215.
34. Skirrow G (1975) The dissolved gases: Carbon dioxide. *Chemical Oceanography*, eds Riley JP, Skirrow G (Academic, San Diego), Vol 2, pp 1–92.
35. Riley WJ, Still CJ, Torn MS, Berry JA (2002) A mechanistic model of $H_2^{18}O$ and $CO^{18}O$ fluxes between ecosystems and the atmosphere: Model description and sensitivity analysis. *Global Biogeochem Cycles*, 1010.1029/2002GB001878.

GEOPHYSICS

MICROBIOLOGY